

Implantable Pulse Oximetry on Subcutaneous Tissue

Michael Theodor¹, Dominic Ruh¹, Sivaraman Subramanian¹, Katharina Förster²,
Claudia Heilmann², Friedhelm Beyersdorf², Dennis Plachta¹, Yiannos Manoli¹, *Member, IEEE*,
Hans Zappe¹, *Member, IEEE*, and Andreas Seifert¹

Abstract—Blood oxygen saturation is one of the most prominent measurement parameters in daily clinical routine. However up to now, it is not possible to continuously monitor this parameter reliably in mobile patients. High-risk patients suffering from cardiovascular diseases could benefit from long-term monitoring of blood oxygen saturation. In this paper, we present a minimally invasive, implantable patient monitor which is capable of monitoring vital signs. The capability of this multi-modal sensor to subcutaneously determine blood pressure, pulse and ECG has been demonstrated earlier. This paper focuses on monitoring of blood oxygen saturation. Even though the signal amplitudes are much weaker than for standard extracorporeal measurements, photoplethysmographic signals were recorded with high quality *in vivo* directly on subcutaneous muscle tissue. For the first time, it has been shown that blood oxygen saturation can be measured with an implantable, but extravascular sensor. The sensor was implanted for two weeks in a sheep and did not cause any complications. This opens new perspectives for home monitoring of patients with cardiovascular diseases.

I. INTRODUCTION

Telecardiology, as a new enabling technology for monitoring vital signs outside clinical environment has proven to reduce mortality in comparison with standard care [1].

Common symptoms of heart failure are dyspnea and low arterial oxygen saturation (hypoxemia). Therefore, it is suggested to monitor arterial oxygen saturation of corresponding patients over the long-term [2]. Pulse oximetry is an established method to measure arterial oxygen saturation and has been used in clinical practice for more than two decades [3]. However, by state-of-the-art methods, continuous monitoring of mobile patients is not possible.

Recently, we have published a multi-modal system featuring an optical blood pressure sensor to be placed subcutaneously [4]. Now, we expand its capabilities by including pulse oximetry thereby providing an implantable medical monitor with higher functionality.

Within this paper, we present the first pulse oximeter which is implanted on subcutaneous tissue and makes continuous monitoring possible. The next section summarizes firstly the general theory of pulse oximetry and then describes the special challenge of operating the sensor on subcutaneous tissue. Section III presents the design of the sensor as well as the optical simulation of photons in tissue for this geometry.

¹ Authors are with the Department of Microsystems Engineering, University of Freiburg, Georges-Koehler-Allee 102, 79110 Freiburg, Germany

² Authors are with the Heart Center Freiburg University, Hugstetter Strasse 55, 79106 Freiburg, Germany

Y. Manoli is additionally with HSG-IMIT, Wilhelm-Schickard-Strasse 10, 78052 Villingen-Schwenningen, Germany

michael.theodor@imtek.uni-freiburg.de

The sensor is evaluated *in vivo* measuring blood pulses and oxygen saturation inside an animal under narcosis, which is shown in Section IV.

II. BACKGROUND

A. Pulse Oximetry

Oxygen transport in the body is performed by the metalloprotein hemoglobin, which is a strong light absorber. Within the arterial blood of a healthy human, ca. 99 % of the hemoglobin molecules are oxygenated. The arterial oxygen saturation SaO_2 can be measured by pulse oximetry.

A pulse oximeter is an optical sensor which, as shown in the inset in Fig. 1, transmits light at red and infrared wavelengths into well-perfused tissue and measures transmitted or, as in our case, reflected intensities [5].

The absorption of arterial blood causes a pulsating component in the measured signal which is called photoplethysmogram (PPG) and delivers the characteristic shape of a blood pressure pulse. The PPG can also be used to determine pulse transit time which is correlated with blood pressure as shown for example in [4], [6], [7].

Oxygenated and deoxygenated blood have different absorption spectra. Pulse oximeters use red light, which is strongly absorbed by deoxygenated blood, and light in the infrared region, where oxygenated blood shows stronger absorption. The presented sensor uses light at 660 nm and 935 nm. To determine SaO_2 and to extract absorption solely caused by arterial blood, we use the so-called ratio of normalized intensities

$$R = \frac{\ln(I_{red,max}/I_{red,min})}{\ln(I_{ir,max}/I_{ir,min})}, \quad (1)$$

where I_x is the maximum/minimum intensity in the red/infrared light of each single pulse. This formula is based on Lambert-Beer's law [5]. Empiric 1st order calibration curves in the form of

$$SaO_2 = mR + c, \quad (2)$$

with slope m and offset c , have proven to give a good SaO_2 approximation in the physiologically relevant range for measurements at the finger [8]. For the utilized wavelengths, the empirically determined parameters for human skin are $m = -26\%$ and $c = 110\%$ [8].

B. Conditions on Subcutaneous Tissue

In contrast to all other oxygen sensing approaches, we measured the pulse oximetric signals directly on muscle tissue. The sensors were positioned at the neck part of the

musculus trapezius and at the nearby musculus cleidooccipitalis of a sheep. As shown in Figure 2, these muscles provide enough space for an implant. In contrast to leg muscles, the neck muscles are predominantly responsible for stabilization and slower movements. Measurements which take place during rapid movements will be subject to significant motion artifacts. Both, the m. trapezius and the m. cleidooccipitalis are striated muscles and consist of mainly slow oxidative fibers. Blood perfusion of subcutaneous tissue is generally weaker than in the finger-tip or ear-lobe, where conventional pulse oximeters are applied. [9]

The volume fraction of arterial blood in a muscle is ca. 1.5%, but displays a strong variation, dependent on training level, kind of muscle, gender and age. Muscles are surrounded by the fascia, which is a thin layer of several microns of connective tissue, consisting mainly of collagen fibers. The fascia does not contain blood vessels and exhibits optical scattering more than 10 times stronger than muscle tissue, hence decreasing PPG signal strength. [10]

A significant difference between sheep and human blood is the hematocrit. Whereas healthy sheep show hematocrit levels of 25–35%, humans exhibit values of 37–50%. [11]

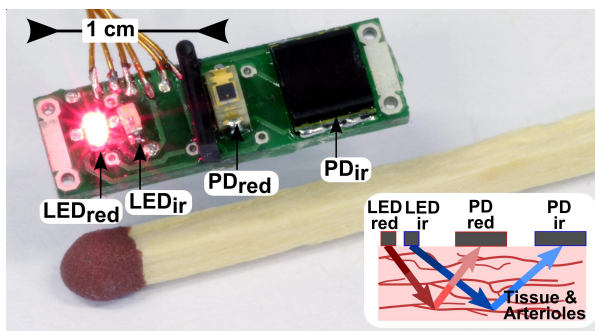


Fig. 1. Implantable reflective pulse oximeter. The light transmitters (LED) and receivers (PD) for red and infrared light are separated by a barrier. The inset on the right shows the principle of reflective pulse oximetry.

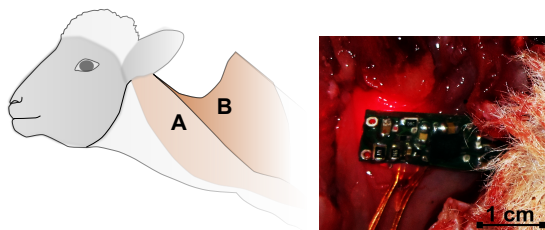


Fig. 2. **Left:** Implant positions on muscle tissue of a sheep. A: musculus cleidooccipitalis, B: musculus trapezius. **Right:** Photograph of the subcutaneously placed pulse oximeter.

III. SENSOR

A. Design

The sensor used for the measurements is a reflection mode pulse oximeter. Fig. 1 shows the front of the sensor, which consists of two pairs of a photodiode and a light emitting diode (LED) for red (660 nm) and infrared (935 nm)

light, respectively. Conventional pulse oximeters use only one photo detector and separate the two wavelengths by switching [8]. This sensor concept features two photodiodes with narrow spectral bandwidth, which are sensitive only to light of the wavelength of one of the LEDs, thereby avoiding crosstalk and suppressing disturbances from ambient light. This concept allows continuous operation of the LEDs without switching and hence less distorted signals.

Both photo diodes have similar sensitivities of 0.4 A/W, but the active area of the infrared detector is, with 7.5 mm², 11 times larger. Driven at currents of 20 and 30 mA, the optical power density of the red and infrared LED is 2.4 mW/sr and 1.8 mW/sr, respectively, with a beam angle of 120°. The optimal signal quality has been determined empirically by an experimental series for a spacing between transmitter and receiver of 10 mm for infrared and 7 mm for red light.

A dual transimpedance amplifier is integrated directly on the backside of the sensor to realize short track lengths and minimize electrical interference between the weak sensor signal and the amplifier. By using two photodiodes in close proximity to the amplifier, the signal-to-noise ratio increases significantly, thereby compensating the drawback of weaker signals derived from muscle tissue. For protection against moisture, the pulse oximeter is coated by a 10 μm Parylene C layer, which is a standard coating for cardiac pacemakers. Covered in transparent, biocompatible MED-1000 silicone, the sensor's total dimensions are 18 × 6 × 2 mm³.

This packaging allows operation over several months. To extend implant lifetime, a hermetic package has to be employed. This can be based on sapphire, as transparent ceramics, with a metal lid, which has already shown to provide good long-term biocompatibility [12]. The implant can be powered by a rechargeable 3.7 V Li-ion battery.

B. Simulation

To visualize the photon propagation in tissue, a numerical simulation was applied. The algorithms are based on a method developed by Wang et al. and modified by Ruh et al. [13], [14] and simulate radiative transfer in biological media using the Monte Carlo method.

The Monte Carlo approach simulates the path of 10⁸ photons through a layer of blood-perfused tissue with the empirical optical properties from [15]. The volume fraction of the arterial blood is assumed to be 1%.

The plot in Fig. 3 shows the probability density function of photons on their path from the source to the detector. The plot displays only those photons which arrive at the detector. The corresponding fractions are 0.15% for IR light and 0.025% for red light. The deviation can be explained by the detector area which is significantly larger for infrared light.

The distances between emitter and detector were chosen such that the penetration depths are similar for the two wavelengths. The corresponding calculated mean depths are 2.3 mm for red and 2.8 mm for infrared light. The most probable optical path is indicated by the black lines in Figure 3 with maximum depths of 1.5 mm for red and 1.8 mm for infrared light.

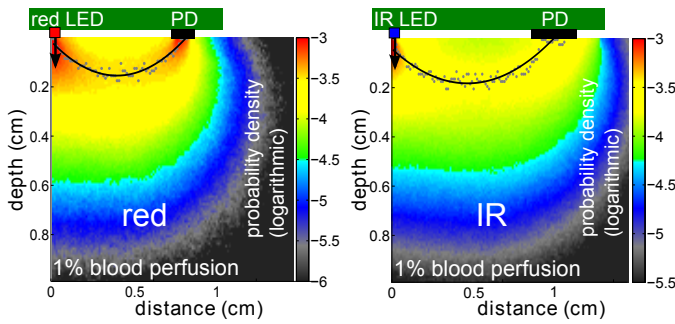


Fig. 3. Monte Carlo simulation of the photon flux density in muscle tissue containing 1% volume fraction of arterial blood. The plot shows the probability density function of optical paths taken by the photon packets from source to detector. The black line shows the photon path with the highest probability and shows a maximum depth of 1.5 mm for red and 1.8 mm for infrared light.

IV. IN VIVO RESULTS

To prove its function, the sensors were evaluated during surgery on a domestic sheep, thereby placed on the neck-part of the m. trapezius and on the m. cleidocapitalis. The m. latissimus at the back and the intercostal tissue at the thorax have proven to be unsuitable for these measurements due to strong respiration artifacts and weaker signal strength.

The animal was set under narcosis with propofol and heparine. Changes in SaO_2 were caused by stopping the artificial respiration machine for 90 s. As reference, a central venous oximetry catheter (CeVOX) was inserted into the femoral artery for continuous monitoring. The CeVOX was calibrated for the sheep by blood gas analysis of arterial blood samples.

Animal experiments (registration code G-10/67) were approved by the local ethics committee (Freiburg, Germany) and performed in accordance with the rules and regulations of the German animal protection law and the animal care guidelines of the European Community (86/609/EC).

A. Photoplethysmographic Signals

The sensor was able to detect PPG signals with high quality with similar DC intensities for all measurements from the anaesthetized animal. The ratio of the alternating (AC) and constant (DC) parts of the PPG on sheep muscles is 0.03–0.14% and lower than the values measured extracorporeally, due to reduced capillary density of the muscle tissue.

Despite such small signal amplitudes, the sensor was able to measure the blood pulse curve with high resolution. The magnified signal, shown in Fig. 4, exhibits details that make the sensor suitable for pulse wave analysis and pulse transit time determination.

Figure 5 shows the power spectral density of the PPG signal acquired subcutaneously. The clearly visible peaks allow an exact determination of the respiration frequency as well as the heart rate. The first peak at 0.285 Hz coincides with the artificial respiration frequency of 17/min. The heart rate of 92/min, determined by an ECG as reference, agrees with the second peak in Figure 5 at 1.53 Hz. Other dominant peaks at 3.1, 4.6, 6.1, 7.7 and 9.2 Hz are clear multiples of the

heart rate and thus overtones of the pulse. Determined with this high quality, the overtones contain valuable information for pulse wave analysis [6].

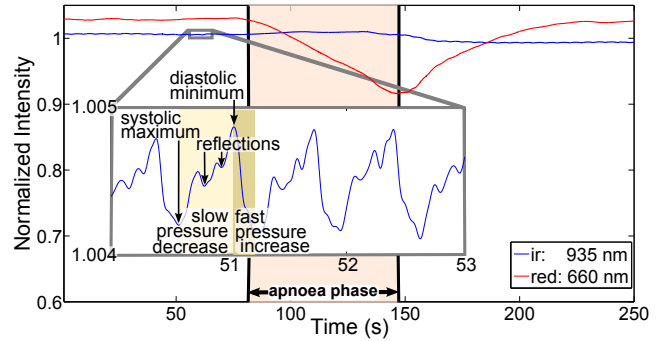


Fig. 4. Detected intensity of reflected red and infrared light during blood oxygen variation down to a saturation of 65% for the animal under narcosis. The vertical lines indicate start and stop of the apnoea phase. The inset in the lower left magnifies 3 s of the IR PPG measurement and shows 4 pulses with their characteristic form, namely a slow intensity increase with falling pressure and quick decrease with systolic slope.

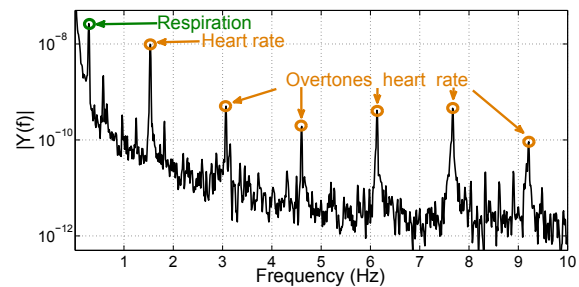


Fig. 5. Power spectral density of the red PPG signal from subcutaneous tissue at rest over 1 minute with an exact determination of the respiration frequency of 0.285 Hz (17/min) and the heart rate of 1.54 Hz (92/min) with 5 overtones.

B. Pulse Oximetry

All oxygen sweeps taken at both muscles show the same behavior. Red light faces a 6 times higher absorption for deoxygenated than for oxygenated hemoglobin. Therefore, this signal decreases with lower oxygen saturation, as seen in Fig. 4, while the infrared signal rises slightly.

Fig. 6 shows the ratio of normalized intensities R calculated from the intensities in Fig. 4 using Eq. 1. According to theory, R and the blood oxygen saturation show a linear trend. The two values agree with a high Pearson's correlation coefficient of $r = 0.97$. The determined coefficients for Eq. 2 are $m_{sheep} = -26\%$ and $c_{sheep} = 96\%$. The slope m agrees with the human value, whereas c differs by 14%. This deviation can be explained by physiological differences, in particular the lower hematocrit level of sheep.

With the determined coefficients m_{sheep} and c_{sheep} , the blood oxygen saturation can be calculated from the measured pulse oximetric data. Fig. 7 shows the intra-arterially acquired reference in comparison with the SaO_2 values measured by our minimally invasive method. The figure

clearly shows, that the implantable pulse oximeter is capable of detecting an apnoea phase. The oxygen saturation has been varied three times. Temporal delays between reference and implant are in the region of one heart beat and, therefore, not visible in Fig. 7. The reference and measurement values agree with correlation coefficients of 0.97, 0.96 and 0.92, respectively. The corresponding standard deviations are 3.8, 4.0 and 6.7 %. This corroborates the high accuracy of detecting blood oxygen saturation on subcutaneous tissue with the developed sensor.

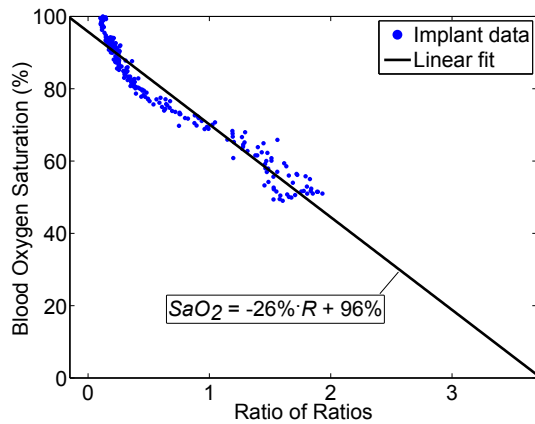


Fig. 6. The plot shows the intra-arterial reference SaO_2 values over the PPG-determined ratio of normalized intensities R calculated by Eq. 1. According to theory, the values show a linear relation with a correlation coefficient of 0.97.

C. Biocompatibility Test

To evaluate biocompatibility, a passive sensor was autoclaved and implanted subcutaneously in a sheep over two weeks without any complications. The animal recovered quickly from surgery and displayed – under observation and care of experienced veterinarians – normal, apparently pain-free behavior, from the first day after operation. After two weeks, the sensor was explanted and did not show any impairment or damage, still fully functional.

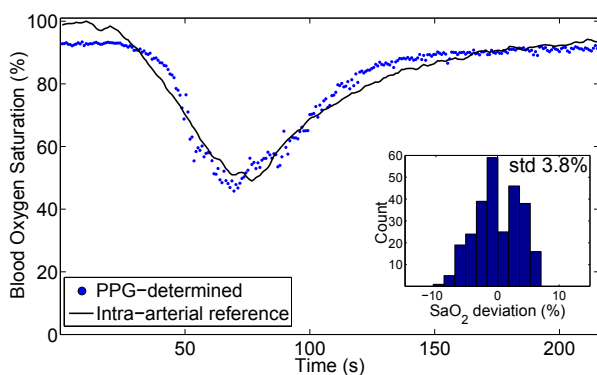


Fig. 7. Measured SaO_2 with the new sensor during an apnoea phase of 90s compared to intra-arterial reference data. The histogram on the right shows the deviation between measurement and reference with a standard deviation of 3.8 %.

V. CONCLUSION

It has been shown that photoplethysmograms can be acquired with high quality on subcutaneous muscle tissue. For the first time, arterial oxygen saturation could precisely be measured with an implantable, but extravascular sensor. Calculated values fit linearly with high correlation to the intra-arterial reference. Additionally, the optical signal delivers heart rate and respiration frequency. To prove biocompatibility, the sensor has been implanted over two weeks with only a small, minimally invasive incision and did not cause any complications. Combined with a method, presented previously, to estimate blood pressure via pulse transit time, the system will serve as a multi-modal medical monitor, enabling new perspectives for telecardiologic monitoring of patients with cardiovascular diseases.

ACKNOWLEDGMENT

The author would like to thank Gerda and Dr. Fritz Ruf and the Fritz-Hüttinger-Foundation for financial support.

REFERENCES

- [1] G. Boriani, I. Diemberger, C. Martignani, M. Biffi, C. Valzania, M. Bertini, G. Domenichini, D. Saporito, M. Ziacchi, and A. Branzi, "Telecardiology and remote monitoring of implanted electrical devices: The potential for fresh clinical care perspectives," *Journal of General Internal Medicine*, vol. 23, pp. 73–77, 2008.
- [2] A. Mortara, L. Bernardi, G. Pinna, G. Spadacini, R. Maestri, M. Dambacher, C. Muller, P. Sleight, L. Tavazzi, H. Roskamm, and A. Frey, "Alterations of breathing in chronic heart failure: clinical relevance of arterial oxygen saturation instability," *Clinical Science*, vol. 91, pp. 72–74, 1996.
- [3] V. A. Potter, "Pulse oximetry in general practice: How would a pulse oximeter influence patient management?" *European Journal of General Practice*, vol. 13-4, pp. 216–220, 2007.
- [4] M. Theodor, D. Ruh, J. Fiala, K. Foerster, C. Heilmann, Y. Manoli, F. Beyersdorf, H. Zappe, and A. Seifert, "Subcutaneous blood pressure monitoring with an implantable optical sensor," *Biomedical Microdevices*, vol. 15-5, pp. 811–820, 2013.
- [5] J. G. Webster, *Design of Pulse Oximeters*, J. G. Webster, Ed. Institute of Physics Publishing, 1997.
- [6] P. Salvi, *Pulse Waves*. Springer Milan, 2012.
- [7] J. Fiala, P. Bingger, D. Ruh, K. Foerster, C. Heilmann, F. Beyersdorf, H. Zappe, and A. Seifert, "An implantable optical blood pressure sensor based on pulse transit time," *Biomedical Microdevices*, vol. 15, pp. 73–81, 2013.
- [8] J. Moyle, *Pulse Oximetry*. BMJ Books, 2002.
- [9] P. Popesko, *Atlas of Topographical Anatomy of the Domestic Animals*, 2, Ed. W B Saunders Co., 1978.
- [10] C. P. Pfeffer, B. R. Olsen, , and F. Legare, "Second harmonic generation imaging of fascia within thick tissue block," *Optics Express*, vol. 15 (12), pp. 7296–7302, 2007.
- [11] P. Dooley and V. Williams, "Changes in the jugular haematocrit of sheep during feeding," *Australian Journal of Biological Science*, vol. 28, pp. 43–53, 1975.
- [12] M. Schuettler, J. Ordonez, T. Santisteban, A. Schatz, J. Wilde, and T. Stieglitz, "Fabrication and test of a hermetic miniature implant package with 360 electrical feedthroughs," in *32nd Annual International Conference of the IEEE EMBS, 1585-1588*, 2010.
- [13] L. Wang, S. Jaques, and L. Zheng, "Mcm1 - monte carlo modeling of light transport in multi-layered tissues," *Computer Methods and Programs in Biomedicine*, vol. 47, pp. 131–146, 1995.
- [14] D. Ruh, S. Subramanian, M. Theodor, H. Zappe, and A. Seifert, "Radiative transport in large arteries," *Biomedical Optics Express*, vol. 5(1), pp. 54–68, 2014.
- [15] J. M. Schmitt, "Simple photon diffusion analysis of the effects of multiple scattering on pulse oximetry," *Transactions on Biomedical Engineering*, vol. 38, pp. 1194–1203, 1991.